A RADARSAT-2 Quad-Polarized Time Series for Monitoring Crop and Soil Conditions in Barrax, Spain

M. Susan Moran, Luis Alonso, Jose F. Moreno, Maria Pilar Cendrero Mateo, D. Fernando de la Cruz, and Amelia Montoro

***Abstract*—An analysis of the sensitivity of synthetic aperture radar (SAR) backscatter (σ^o) to crop and soil conditions was conducted using 57 RADARSAT-2 C-band quad-polarized SAR images acquired from April to September 2009 for large fields of wheat, barley, oat, corn, onion, and alfalfa in Barrax, Spain. Preliminary results showed that the cross-polarized σ^o_{HV} was particularly useful for monitoring both crop and soil conditions and was the least sensitive to differences in beam incidence angle. The greatest separability of barley, corn, and onion occurred in spring after the barley had been harvested or in the narrow time window associated with grain crop heading when corn and onion were still immature. The time series of σ^o offered reliable information about crop growth stage, such as jointing and heading in grain crops and leaf growth and reproduction in corn and onion. There was a positive correlation between σ^o and the Normalized Difference Vegetation Index for onion and corn but not for all crops, and the impact of view direction and incidence angle on the time series was minimal compared to the signal response to crop and soil conditions. Related to planning for future C-band SAR missions, we found that quad-polarization with image acquisition frequency from 3–6 days was best suited for distinguishing crop types and for monitoring crop phenology, single- or dual-polarization with an acquisition frequency of 3–6 days was sufficient for mapping crop green biomass, and single- or dual-polarization with daily image acquisition was necessary to capture rapid changes in soil moisture condition.**

***Index Terms*—Barley, corn, onion, phenology, Radarsat, Rapideye, Sentinel-1.**

Manuscript received September 30, 2010; revised June 20, 2011; accepted July 31, 2011. This paper is the direct result of a fellowship funded by the OECD Co-operative Research Programme: Biological Resource Management for Sustainable Agricultural Systems to encourage international research on sustainable use of natural resources in agriculture. This work was supported in part by the Spanish Ministry for Education and Science under projects EODIX/AYA2008-05965-C04-03 and CONSOLIDER/CSD2007-00018 and the NASA SMAP Science Definition Team under agreement 08-SMAPSDT08-0042. Special thanks go to the European Space Agency for providing the AgriSAR 2009 data set.

M. S. Moran is with the USDA Southwest Watershed Research Center, Tucson, AZ 85719 USA (e-mail: susan.moran@ars.usda.gov).

L. Alonso, J. F. Moreno, and M. P. Cendrero Mateo are with the Image Processing Laboratory, University of Valencia, 46980 Valencia, Spain (e-mail: lalonso.uv@gmail.com; moreno.uv@gmail.com; macenma@email.arizona.edu).

D. F. de la Cruz and A. Montoro are with the Instituto Técnico Agronómico Provincial (ITAP), 02080 Albacete, Spain (e-mail: fct.itap@dipualba.es; meli.itap@dipualba.es).

Color versions of one or more of the figures in this paper are available online at http://ieeexplore.ieee.org.

Digital Object Identifier 10.1109/TGRS.2011.2166080

I. Introduction

IT HAS long been recognized that satellite imagery has a unique and important role in monitoring crop and soil conditions for farm management [27]. Most studies of satellite imagery for crop monitoring have focused on the use of optical imagery using the reflectance of visible and NIR radiation (wavelength $(\lambda) \sim 0.4{-}1.1$ μm) and the emittance of thermal IR radiation ($\lambda \sim 8{-}12$ μm) to map characteristics over large areas [24]. However, longer microwave wavelengths ($\lambda \sim 1.7{-}30$ cm) have some important advantages over optical remote sensing for agricultural applications. Perhaps the most valuable advantage is the ability of the microwave signal to pass through the atmosphere and clouds with negligible attenuation, thus allowing frequent repeat measurements over the short dynamic growing season of crops. Recent satellites supporting synthetic aperture radar (SAR) sensors offer the added advantages of fine resolution (on the order of 10 m), day and night coverage, multiple polarimetric modes, variety of beam incidence angles, and acquisitions to either the left or right of the satellite track. The RADARSAT-2 satellite system with C-band SAR ($\lambda \sim 5.5$ cm) offers all of these specifications (Table I; [44]). For these reasons, there is great interest in using RADARSAT-2 for research on application of SAR imagery for determining crop and soil condition, including monitoring crop biomass, leaf area, crop residue, plant water content, crop growth stage, soil tillage, and soil water content [11], [35].

However, even with the availability of RADARSAT-2 images, research will be constrained by the common disadvantages of satellite measurements of radar backscatter. Although SAR imagery is acquired at fine resolution, it requires a correction for inherent speckle that often results in operational resolution on the order of hundreds rather than tens of meters [59]. Thus, cropped fields must be large (on the order of 1 km^2) to match the coarse spatial resolution of speckle-corrected SAR data. Studies designed to track crop conditions based on frequent RADARSAT-2 SAR acquisitions will be faced with the challenge of disentangling the signal associated with different sensor view directions and beam incidence angles from that associated with day-to-day changes in crop/soil conditions. Thus, to arrive at conclusive results, studies must be designed to include intensive ground-based measurements of multiple crops and soils. Finally, total radar backscatter is a complex sum of the backscatter from vegetation and soil, where

TABLE I
RADARSAT-2, RAPIDEYE, AND SENTINEL-1 SATELLITE AND SENSOR CHARACTERISTICS, WHERE NA INDICATES THAT THE CHARACTERISTICS ARE NOT APPLICABLE TO THE SATELLITE OR SENSOR

	RADARSAT-2 (Fine-Quad Mode)	**RapidEye**	**Sentinel-1**
Nominal swath width	25 km	77 km	80 km
Wavelength / frequency	C-Band (5.405 GHz, 5.54 cm)	Blue (0.40-0.51 μm), green(0.52-0.59), red (0.63-0.685), red-edge (0.69-0.73), NIR (0.76-0.85)	C-Band (5.405 GHz, 5.54 cm)
Polarization	Full quad - polarization HH+VV+HV+VH	NA	Selectable dual polarization (VV+VH or HH+HV)
Beam Incidence Angles	20-41°	NA	20-41°
Approx. Ground Resolution	Acquired 5.4-8 m, resampled for AgriSAR to 20 m	5 m	5 m
Repeat cycle	24 days at one satellite/sensor configuration; Average every 3 days using multiple satellite/sensor configurations	Daily, using a constellation of 5 satellites	Two days, using a constellation of satellites (two minimum) and multiple satellite/sensor configurations
Mission life	Designed for 7-yr operational life		Designed for 7.5-yr operational life
Launch Date	December 2007	August 2008	2011

the radar beam can penetrate both the canopy and soil to a difficult-to-determine depth, making it complicated to determine if the signal is dominated by the crop or soil conditions. Again, reliable ground measurements of crop growth stage and daily irrigation and precipitation throughout the growing season are key to a successful investigation.

Because of these constraints, there have been few studies with a dense time series of radar backscatter measurements over multiple crops throughout the growing season with sufficient *in situ* crop and soil measurements to interpret the results for farm management. Most studies are based on interpretation of < 15 satellite images taken with the same sensor configuration over the growing season [5]–[8], [32], [53], [61], [65]. Ground measurements of crop and soil conditions are often lacking in such regional studies, and the focus is generally on mapping crop type rather than condition. Excellent studies have been conducted with ground-based boom-mounted radar scatterometers deployed to make daily measurements over a single crop through the growing season (e.g., [34], [46], and [62]). Unfortunately, such ground-based systems are rare (due to the high cost of the system and its deployment), and they are generally limited to local deployment with measurements over few crop types per year. Nonetheless, these rich season-long data sets of multiband, multipolarized, and multitemporal measurements have provided our general understanding of radar backscattering from crops and soils and have been the basis for nearly all radar backscatter modeling. However, we are still uncertain of the effects of polarization, frequency, incidence angle, and view direction as a function of crop type, density, and development stage [23].

Generally, we know that a dense time series of linear quad-polarized images would increase the dimensionality of the radar data set and improve our ability to monitor both crop and soil conditions. Regarding crop type separability, a time series of C-band radar images has produced results more accurate than those obtained with a single C-band radar image [7], [16], [19], [26], [52], [54], [58], [65]. Fewer images are required if the image acquisition is synchronized with the crop calendar [6], [12], [28], [37], [52]. The differential attenuation of grain crops in linearly copolarized response (HH versus VV) and the ratio (or difference) of the copolarized radar backscatter $\sigma^o_{\mathrm{VV}}/\sigma^o_{\mathrm{HH}}$ (or $\sigma^o_{\mathrm{VV}} - \sigma^o_{\mathrm{HH}}$) have been reported to be useful for discriminating grain crops [64]. However, in other crops (and some growth stages of grain crops), σ^o_{VV} and σ^o_{HH} are well correlated [3], and it has also been reported that the cross-polarization radar backscatter (σ^o_{HV}) was superior to copolarization for crop type separability [14], [18] in part because σ^o_{HV} had the highest dynamic range. Theoretically, grain crops with vertical stem structure lead to double bounce and high σ^o_{VV}; however, their leaves attenuate double bounce and result in more diffuse scatter, like randomly structured crops (e.g., alfalfa). In summary, studies have found that inclusion of multipolarization and multitemporal data improves crop classification, although specific results varied [19], [22], [40], [56], [65].

Regarding crop stage and yield, different polarizations may be most sensitive to crop development at different crop stages, e.g., [29] reported that σ^o_{HH} and σ^o_{VV} were sensitive to different crop conditions in the booting stages of wheat. The linear cross-polarization σ^o_{HV} has been reported to provide the greatest contrast between zones of high and low productivities [3], [35]. Radar signal tends to increase quickly with increasing crop height (biomass) until a threshold height—which depends on crop type, radar polarization, and beam incidence angle—after which the signal increases only slightly [3]. Ferrazzoli *et al.* [21] found that this increase was associated with biomass increases from 0 to 2 kg/m^2 in small-stem crops such as alfalfa. These results are complicated by the fact that the radar signal from freshly ploughed fields with rough soil surfaces can be on the same order as that of mature crops [3]. Like crop classification, results are best when the timing of the image acquisition coincides with critical crop growth phases in the cycle, such as seedling emergence and canopy closure [51]. This is particularly important because the dynamic range related to plant growth is reportedly small, e.g., 8 dB for rice [50] and only 3 dB for potato [48]. With proper timing, SAR images can provide information related to crop yield. McNairn and Brisco

[35] reported that σ^o_{HV} was responsive to zones of higher grain productivity if the image was acquired just weeks prior to crop harvest. They hypothesized that this higher backscatter was due to sensitivity to greater volumetric moisture in the wheat heads.

A time series of linearly quad-polarized images has advantages for mapping soil moisture content as well. The trends in radar backscatter measured on different dates can be correlated with soil moisture content since the effects of spatial roughness variations are smoothed [42], [47], [60]. Balenzano *et al.* [4] reported that a ratio of backscatter measured on two close successive dates might be a simple and effective way to decouple the effect of vegetation and surface roughness from the effect of soil moisture changes when volumetric scattering by the crop canopy is not dominant. While most satellite-based SAR systems are designed to map soil moisture with copolarizations HH or VV, some studies have suggested that cross-polarization could be more sensitive to soil moisture variations [25], [35].

Regarding the inclusion of different sensor configurations (i.e., view direction and incidence angle) in a dense image time series, it is generally accepted that shallow incidence angles $(\theta_i > 40^\circ)$ increase the pathlength through vegetation and maximize the response to crop conditions [3], [9], [15], [17]. Steep incidence angles $(\theta_i < 30^\circ)$ are more useful for soil moisture measurement because they decrease the effects of soil roughness and vegetation attenuation [33]. It has been reported that small changes in incidence angle can have strong impacts on radar backscatter [5] and that a variation with incidence angle was most pronounced in the early season when the backscatter was dominated by surface scattering [55]. The rise in backscatter associated with beam incidence angle can be on the order of several decibels [51]. Radar look direction is also important, particularly relative to row direction. The backscatter from a field viewed with the look direction perpendicular to the row direction can be 5–10 dB higher than the look directions just $5^\circ - 15^\circ$ off perpendicular [13], [41] and can be up to 20 dB in extreme cases [50]. Some studies have reported that the sensitivity to radar look direction effects may be reduced or eliminated for linear cross-polarizations [13], [36].

In this paper, a dense time series of RADARSAT-2 images was acquired over a growing season in a well-instrumented agricultural region coincident with intensive monitoring of crop growth stage, precipitation, and irrigation. The main objective of this paper was to analyze a time series of RADARSAT-2 quad-polarized data to define and quantify the performance of Sentinel-1 and other future European Space Agency (ESA) C-band SAR missions for classifying and monitoring agricultural crops. Multiple university and agency investigators joined to conduct the ESA AgriSAR campaign, where AgriSAR stands for "Agricultural bio/geophysical retrieval from frequent repeat pass SAR and optical imaging" [23]. In 2009, AgriSAR field campaigns were conducted at three locations: Barrax, Spain; Flevoland, The Netherlands; and Indian Head, SK, Canada. In the Barrax region in La Mancha, Spain, 57 RADARSAT-2 C-band quad-polarized SAR images and five RapidEye four-band optical images were acquired from April to September 2009, covering multiple large fields of irrigated and nonirrigated crops. An analysis of the sensitivity of SAR backscatter to crop and soil conditions was conducted using the entire multiview quad-polarized image time series for large fields of corn, barley, wheat, onion, oats, and alfalfa in Barrax. Based on this analysis, suggestions were made for planning the image acquisition frequency and polarimetric mode for the Sentinel-1 mission.

II. Methods

A. Field Site and Ground Measurements

The field campaign was carried out at the Barrax test site and surrounding area. Barrax is located in southeastern Spain on the La Mancha plateau, situated 20 km west of the town of Albacete and about 200 km southeast of the Spanish capital Madrid (centered on 580133.1E 4324867.0N UTM, Zone 30, and Datum WGS84). The test site and surrounding agricultural fields are at an elevation of 700 m, with differences in elevation ranging up to only 2 m. The regional water table is about 20–30 m below the land surface. The Mediterranean climatic conditions result in annual rainfall averages of about 320 mm, with high precipitation in spring and autumn and a minimum in summer. The Barrax test site and surrounding area have been used for agricultural research for many years and are characterized by large uniform land-use units, with some fields measuring 1 km in diameter (Fig. 1). The region consists of approximately 65% dry land and 35% irrigated land, where the main irrigated crops are alfalfa, barley, corn, onion, sugar beet, sunflower, and wheat, and the main means of irrigation are circular pivot sprinkler systems.

Throughout the AgriSAR experiment, records were kept on meteorological conditions, including measurements of air temperature, wind speed and direction, relative humidity (at 2- and 10-m heights), incident and net solar radiation, and reference evapotranspiration (ET_o) in an irrigated field of festuca grass located centrally in the Barrax test site. Meteorological measurements were made by all sensors every 30 s and stored every 10 min. Precipitation amounts were recorded by event start time and duration and also reported as a daily value (P_D in millimeters per day).

Records of irrigation depth (in millimeters per day) applied to cropped fields were kept on a daily basis (I_D). The daily ET_{oD} (in millimeters per day) was measured with a weighing lysimeter of size 2.7 m $\times$ 2.3 m $\times$ 1.7 m deep (as described in detail in [30]), and crop coefficients (k_c) were computed according to Doorenbos and Pruitt [20], deriving field-specific daily consumptive water use (or daily evapotranspiration ET_D), where $ET_D = ET^*_{\mathrm{oD}} k_c$ [1]. A simple field water replenishment estimate for the growing season was computed as $(I_S + P_S)/(ET_S)$, where I_S, P_S, and ET_S are the seasonal sums of I_D, P_D, and ET_D, and the season is defined as the period from field planting to harvest. Thus, a value of 1.0 estimates a seasonal water replenishment close to 100% (Table III).

Beginning in July of the AgriSAR campaign, measurements were made in 23 plots of crop biophysical parameters, including seed density, crop height, and "shadowing area" (plant diameter). For fields both within and surrounding the Barrax test

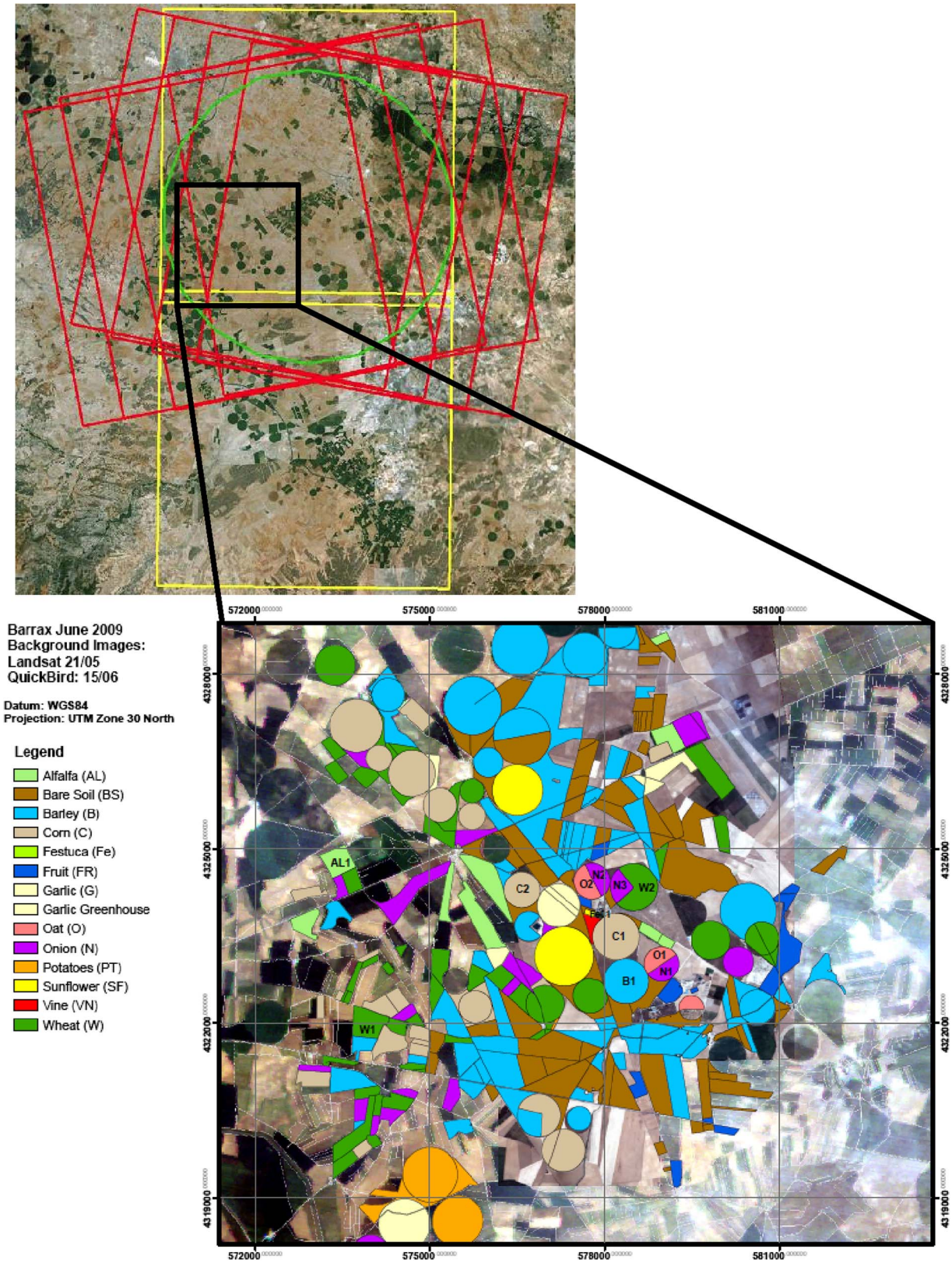

Fig. 1. Location map of the Barrax test site (upper) overlain on a Landsat image, where the red rectangles illustrate the coverage of RADARSAT-2 ascending and descending images at eight different beam incidence angles, the yellow rectangles represent RapidEye coverage, the green circle is the general area of interest, and the black box delineates the Barrax test site for AgriSAR 2009. Map of crop types (lower) in the Barrax study area in June 2009 overlain on Landsat and Quickbird images.

site, crop phenologic stage was recorded, including seedling size, plant development, reproduction stage, and maturation (Table III). Crop type was recorded for all fields in the Barrax region in 2009, resulting in an inventory including alfalfa, barley, corn, festuca grass, fruit tree, garlic, oat, onion, potato, sunflower, and wheat (Fig. 1).

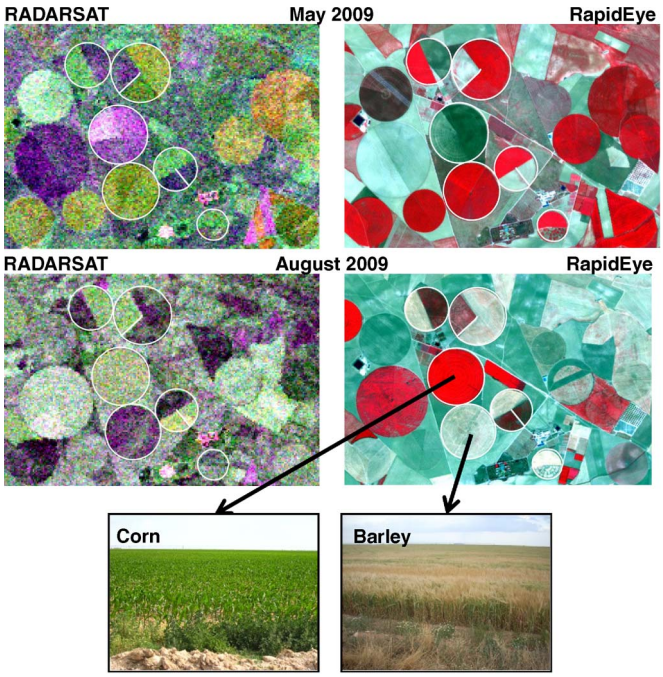

Fig. 2. Sample images of RADARSAT-2 (HH, HV, VV, and RGB) and RapidEye (color composite) in May and August 2009 for an area extracted over the fields in Barrax. The photographs of corn and barley were taken on the ground in July 2009.

B. Image Processing—RADARSAT-2 and RapidEye

Using ascending and descending RADARSAT-2 orbits and beam incidence angles ranging from 23° to 41°, SAR images were acquired on average every 3 days during the AgriSAR experiment from May to August (Fig. 2 and Table II). Ascending (6 P.M.) and descending (6 A.M.) pass acquisitions occurred 12 h apart on consecutive days. For the AgriSAR experiment, RADARSAT-2 fine-quad mode images were resampled to images of backscatter (in decibels) with 20-m spatial resolution and polarizations of HH, HV, and VV under the conventional assumption that HV and VH backscatter would be similar. The RADARSAT-2 absolute radiometric error (average radiometric level offset relative to an outside reference) is reported to be < 0.25 dB, and the relative radiometric error (total radiometric level variations within an image) is reported to be < 0.6 dB [57].

RapidEye images were acquired on multiple dates during the AgriSAR campaign, and five RapidEye images acquired with clear sky conditions were processed for this analysis. An image of Normalized Difference Vegetation Index (NDVI) was derived from the RapidEye five-band imagery, where $NDVI = (L_{\mathrm{NIR}} - L_{\mathrm{Red}})/(L_{\mathrm{NIR}} + L_{\mathrm{Red}})$, $L =$ radiance (in watts per meter steradian micrometer) measured by the calibrated RapidEye sensor, and subscripts Red and NIR refer to RapidEye red (0.63–0.685 μm) and near-infrared (0.76–0.85 μm) wavelength bands. RapidEye imagery was obtained during the AgriSAR campaign for the sole purpose of validating SAR-derived information.

The 5-m resolution RapidEye images were registered to an orthoregistered photo, and subsequently, the RADARSAT-2 images were registered to this georegistered RapidEye image with a second-order fit to within 20-m accuracy. To minimize SAR speckle and to maximize the signal/noise ratio, RADARSAT-2 backscatter was averaged over polygons corresponding to fields of alfalfa, barley, corn, onion, oat, and wheat (Table III). The number of pixels averaged for these polygons ranged from 124 for the smallest field to 1096 for the largest field, related to field sizes from 0.05 to 0.5 km^2. These field sizes correspond well with the optimal ground resolution suggested by [59] for parameter retrieval from SAR images. RapidEye NDVI was averaged over the same polygons on the five dates of RapidEye acquisitions.

These 12 field-scale extracts covering six crops from RADARSAT-2 and RapidEye images formed the data set analyzed in this paper. Although the data for all 12 fields were not reported in the figures to reduce redundancy and to simplify presentation, the results for all 12 fields contributed to the analysis and were consistent with the conclusion.

C. Correlation Analysis for Evaluating Image Acquisition Frequency

To evaluate the similarity in information content between different acquisition frequencies, we computed the correlation coefficient (R^2) between a spline fit of σ^o values measured with an average n-day frequency with a spline fit of σ^o_{HV} values with an average m-day frequency over a given time period for multiple crops. This approach deserves some explanation here to allow proper interpretation in the results section. First, we refer to "average n-day frequency" because the acquisitions are not on a regular n-day frequency (varying 2–3 days from a regular n-day interval) over the study period (see Table II). In this analysis, care was taken to select satellite/sensor configurations that best mimicked a regular n-day frequency (Table IV). Second, because the images were necessarily acquired on different days (Table II), the time periods used for the analysis of n-day frequency varied slightly (Table IV). Thus, the results of the analysis assessed changes in image acquisition *frequency* as well as image acquisition *timing*. This was advantageous since both the number and timing of image acquisitions should be considered in planning the image acquisition frequency for new satellite missions. Finally, the analysis for the alfalfa field differed from all others because the field was not covered by the RADARSAT-2 images acquired with $\theta_i = 40°$ or 41°. These aspects of the analysis have been noted and accommodated in the results and discussion.

III. Results and Discussion

Trends in σ^o over the crop growing season at Barrax were defined by crop type, phenology, irrigation, and precipitation (exemplified by σ^o from fields of barley, corn, and onion in Fig. 3). The highest σ^o at all polarizations was associated with the period in which the crop green biomass generally reaches its maximum for the winter-crop barley (irrigated from day of year DOY 71–179) and the summer-crops corn (irrigated DOY 133–261) and onion (irrigated DOY 68–244). Changes in plant structure associated with crop growth and harvest dictated the overall trend in σ^o, where σ^o was lowest during periods when fields were bare or sparsely vegetated, σ^o increased sharply during crop green-up or decreased abruptly with harvest, and σ^o reached a plateau during crop reproduction. Differences in sensor configuration (orbit and beam incidence angle) had a

TABLE II
AGRISAR 2009 TIME SERIES OF RADARSAT-2 AND RAPIDEYE ACQUISITIONS, WHERE THE DATE IS EXPRESSED AS DAY OF YEAR 2009, THE DSC AND ASC REFER TO DESCENDING AND ASCENDING RADARSAT-2 ORBITS, THE COLUMN HEADERS ARE THE RADARSAT-2 BEAM INCIDENCE ANGLES, AND THE DATES OF RAPIDEYE ACQUISITIONS ARE IN BOLDED BOXES

Pass	**RADARSAT-2 Fine Quad Beam**							
Dsc (6 AM)	**41°**		**25.5°**		**31.2°**		**36.3°**	
Asc (6 PM)		**40°**		**34.3°**		**29°**		**23.2°**
Orbit Cycle	**Day of Year (within 24-day RADARSAT-2 repeat cycle)**							
20		092	093	099	100	106	107	113
21	114	116	117	123	124	130	131	137
22	138	140	141	147	148	154	155	161
23	162	164	165	171	172	178	179	185
24	186	188	189	195	196	202	203	209
25	210	212	213	219	220	226	227	233
26	234	236	237	243				257
27	267	258	260	261	267	268		

TABLE III
DESCRIPTION OF 12 FIELDS SELECTED FOR THIS PAPER AND THE GROUND MEASUREMENTS AVAILABLE FROM MARCH–SEPTEMBER 2009 (DOY 60–273) IN EACH STUDY FIELD. BLANK CELLS INDICATE THAT FIELD INFORMATION IS UNKNOWN OR GROUND DATA ARE NOT ACQUIRED

Description of Study Fields						**Ground Data Available – Day of Year**				
Crop Type & Field Name	**Field Centroid (UTM)**	**Seed Density (plants/m^2)**	**# of Pixels Averaged**	**Row Direction**	**Seasonal Water Replenish-ment Estimate (unitless, defined in text)**	**Irrigation Schedule**	**Phenologic Stage**	**Plant Ht.**	**Plant Diameter**	**Dry Matter & Water Content (kg/m^2)**
Alfalfa1	573503E, 4325032N		555							
Barley1	578443E, 4322912N	308	1023	NNW-SSE		71-179	60-182	172-173		172-173
Barley2	573923E, 4321812N		153			not irrigated				
Corn1	578283E, 4323692N	8	1096	N-S	0.99	133-261	143-264	172 & 188	188	172
Corn2	576663E, 4324492N	10	571					171		172
Onion1	579063E, 4323192N	40	217							
Onion2	577843E, 4324652N	40	124	NE-SW	0.84	72-236	89-235	188	188	
Onion3	578583E, 4324532N	40	234		0.85	68-244	89-235	188	188	
Oat1	579023E, 4323232N		247			74-189	74-196			
Oat2	577823E, 4324612N		281			74-195				
Wheat1	574043E, 4322192N		347			not irrigated				
Wheat2	578623E, 4324512N	523	694	SSW-NNE	0.58	74-187	74-196	171		172

secondary influence on the overall trend and generally resulted in small differences in σ^o relative to the soil/plant-related seasonal trends. Differences in linear co- and cross-polarized radar backscatter appeared to be related to different sensitivities to crop and soil conditions that are explored in the following sections.

A. Crop Condition

Results confirmed that cross-polarized σ^o_{HV} at shallow incidence angles ($\theta_i > 35°$) was more sensitive than σ^o_{HH} to the changes in vegetation structure associated with crop seasonal growth and harvest [Fig. 4(a) and (b)]. The dynamic range of σ^o_{HV} for barley, corn, and onion (11, 9, and 16 dB, respectively) over the growing season was substantially greater than that for σ^o_{HH} (7, 7, and 10 dB). The increase of σ^o_{HV} associated with increased vegetative material in corn and onion fields has been attributed to the depolarizing effect of volumetric scattering within a crop canopy. The highest values of σ^o_{HV} were associated with the densest vegetation canopy for each crop, i.e., during tasseling for corn and bulb growth for onion. The general increase in σ^o associated with corn leaf growth in

TABLE IV
DATE RANGE, SATELLITE/SENSOR CONFIGURATION, AVERAGE IMAGE ACQUISITION FREQUENCIES, AND NUMBER OF IMAGES FOR THE ANALYSES OF IMAGE ACQUISITION FREQUENCY. THE DIFFERENT SATELLITE/SENSOR ORIENTATIONS ARE DEFINED BY THE ORBIT (A: ASCENDING AND D: DESCENDING) AND THE BEAM INCIDENCE ANGLE (RANGING FROM 23° TO 41°)

Dataset for comparison of 3-day versus 24-day image acquisition frequency (multiple configurations versus one configuration)									
Date range	Varied to match the date range for each configuration	113-233	93-213	106-226	100-220	99-219	107-227	92-212	114-234
Satellite/sensor Configuration	All	A23	D25	A29	D31	A34	D36	A40	D41
Average Acquisition Frequency	3-day	24-d	24-d	24-d	24-d	24-d	24-d	24-d	24-d
# of images	41	6	6	6	6	6	6	6	6

Dataset for comparison of 3-day versus 24-day, 12-day, 6-day and 4-day average acquisition frequency					
Date range	Varied to match the date range for each set of configurations	99-219	99-227	93-233	93-233
Satellite/sensor Configuration	All	A34	A34+D36	A34+D36+A23+D25	A34+D36+A23+ D25+A29+D31
Average Acquisition Frequency	3-day	24-d	12-d	6-d	4-d
# of images	41	6	12	24	36

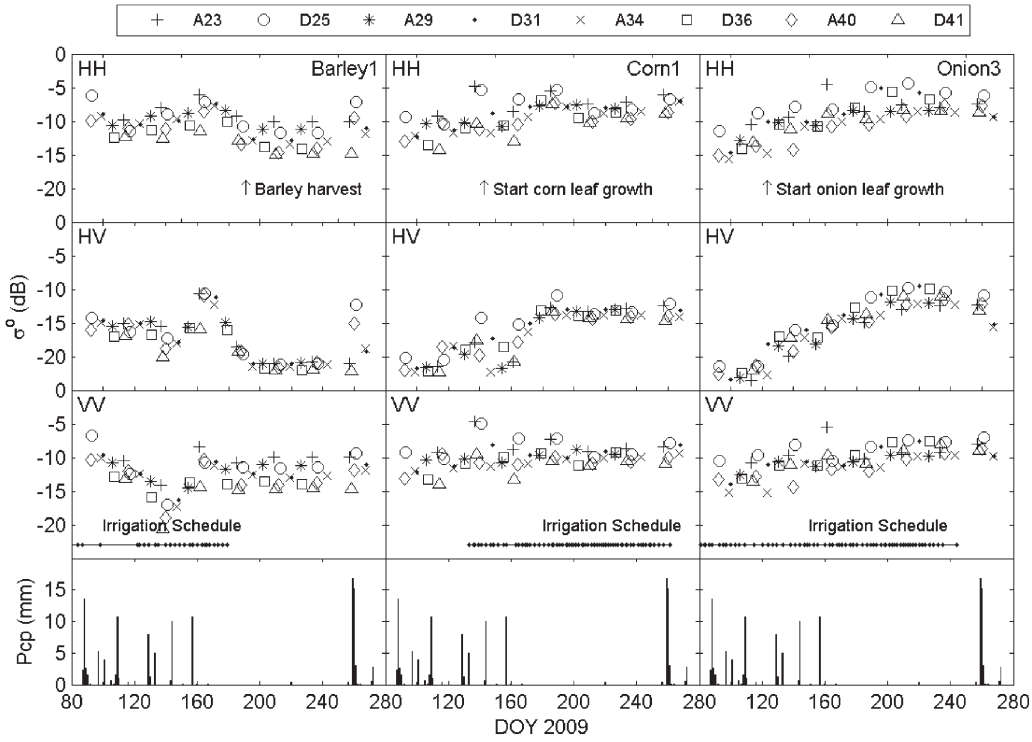

Fig. 3. Radar backscatter values in HH, HV, and VV polarizations for three crops—barley, corn, and onion. The different satellite/sensor orientations are represented by different markers, where the key shows the orbit (A: ascending and D: descending) and the beam incidence angle (ranging from 23° to 41°). The lower panel indicates the precipitation associated with the acquisition dates. The irrigation schedule is indicated by a solid line indicating the temporal extent and by dots indicating the irrigation frequency (the daily irrigation amounts varied, and they are not represented here).

both polarizations may conflict with previous studies reporting no correlation between crop vigor and σ^o for corn [37]. The σ^o_{HV} response for barley was complicated by unique vertical structural characteristics associated with jointing that resulted in an attenuation of the signal in σ^o_{HV} (and σ^o_{VV}) during the period when vegetative material was increasing at a steady rate (as discussed further in the next paragraph).

The difference $\sigma^o_{\mathrm{VV}} - \sigma^o_{\mathrm{HH}}$ was particularly sensitive to the vegetation structure of the grain crop barley. During jointing (when the stem begins to elongate), $\sigma^o_{\mathrm{VV}} - \sigma^o_{\mathrm{HH}}$ became steadily more negative as the σ^o_{VV} signal decreased more than σ^o_{HH} due likely due to signal attenuation with the vertical stem structure of immature grain crops. The dynamic range of $\sigma^o_{\mathrm{VV}} - \sigma^o_{\mathrm{HH}}$ in this barley field was 9 dB from crop emergence

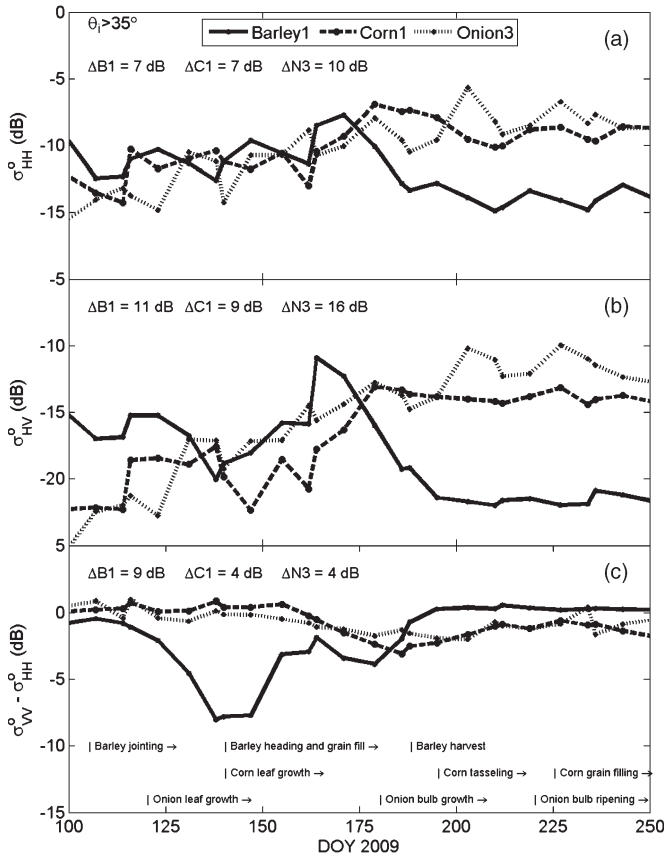

Fig. 4. Radar backscatter values in HH, HV, and VV-HH polarizations for three crops—barley, onion, and corn. The symbols represent the radar backscatter values for measurements made with ascending and descending orbits with beam incidence angles $> 35°$. The crop growth stage is represented with text at the bottom frame of the figure. The dynamic ranges for each crop and polarization are given at the upper left corner of each figure, with abbreviations Barley1 ($\Delta B1$), Corn1 ($\Delta C1$), and Onion3 ($\Delta N3$).

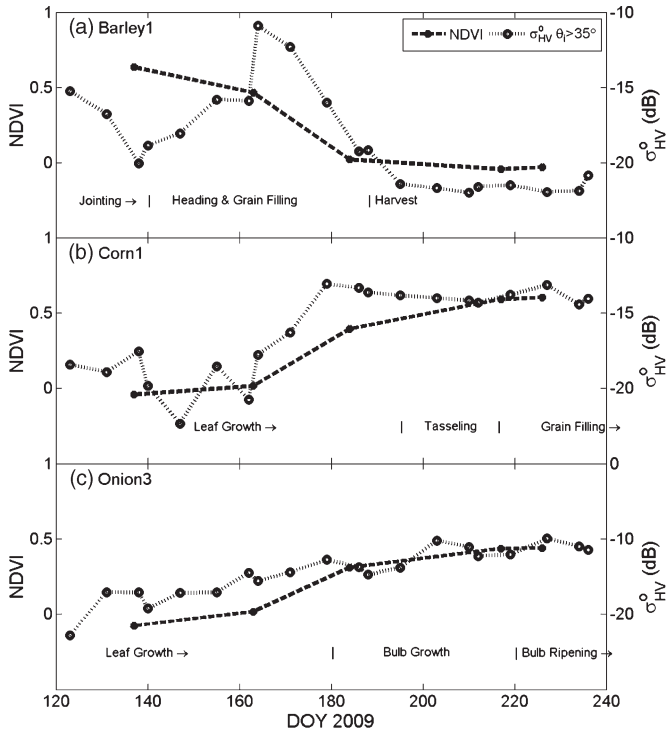

Fig. 5. Radar backscatter values in HV polarization and RapidEye NDVI for three crops. (a) Barley. (b) Corn. (c) Onion. The symbols represent the radar backscatter values for measurements made with ascending and descending orbits with beam incidence angles $> 35°$. The crop growth stage for each crop is represented with text along the bottom of each frame.

through leaf jointing. This $\sigma^o_{\rm VV} - \sigma^o_{\rm HH}$ difference grew smaller (closer to zero) during barley heading and grain filling. There was a similar but less dramatic change in $\sigma^o_{\rm VV} - \sigma^o_{\rm HH}$ associated with leaf growth in corn and onion (dynamic range is 4 dB) and a similar steady decrease in $\sigma^o_{\rm VV} - \sigma^o_{\rm HH}$ with corn tasseling and onion bulb growth.

These distinctive sensitivities of σ^o to vegetation structure should be useful for crop type separability. Other studies have suggested that separability of crop types is best at or near the heading of spring grains and diminishes after the grains have headed and begun to ripen [14], [55]. This is certainly true for separating Barrax barley from corn and onion fields but only when using the $\sigma^o_{\rm VV} - \sigma^o_{\rm HH}$ difference [Fig. 4(c)]. We found that there was a distinctive peak in $\sigma^o_{\rm VV} - \sigma^o_{\rm HH}$ associated with heading in barley (in wheat and oat as well but not shown here) that helped distinguish grain crops from more randomly structured crops such as onion and alfalfa. However, as shown in Fig. 4(c), the results will be most accurate if the image was acquired in the narrow time window associated with crop heading. With single polarizations of $\sigma^o_{\rm HV}$ or $\sigma^o_{\rm HH}$, the greatest separability of barley versus corn and onion occurred in summer after the barley had been harvested [Fig. 4(a) and (b)]. This separability is explained by the dominance of surface scattering for harvested winter crops and volume scattering for lush summer crops.

The relation between $\sigma^o_{\rm HV}$ and crop vegetative growth can be illustrated by comparison of RADARSAT $\sigma^o_{\rm HV}$ with the RapidEye NDVI. Soil moisture and roughness reportedly have little effect on σ^o during the leaf development period [49], [63], and thus, σ^o has been reported to be a surrogate for crop green biomass and to have a strong correlation with NDVI [10], [43], [49]. For corn and onion, there was a striking trend for both $\sigma^o_{\rm HV}$ and NDVI to increase with crop growth [Fig. 5(b) and (c)]. As expected, the NDVI was near zero when the field was fallow or the crop had senesced, the NDVI increased rapidly during stages of green vegetation growth, and the NDVI remained relatively stable during crop reproduction such as barley and corn grain filling and onion bulb ripening. The percentage increase in radar backscatter was on the same order as the percentage increase in NDVI [3]. However, because $\sigma^o_{\rm HV}$ is equally sensitive to leaf water content and canopy structure, its behavior was, at times, different from NDVI. For example, when barley was jointing (stem elongation, as discussed earlier) or producing grain, $\sigma^o_{\rm HV}$ decreased and peaked, respectively, despite a little change in NDVI (or vegetation biomass) associated with these phenologic stages [Fig. 5(a)]. There was no such response to tasseling and reproduction in corn. The smoothest temporal trend in seasonal $\sigma^o_{\rm HV}$ was illustrated for onion, where both NDVI and $\sigma^o_{\rm HV}$ increased rapidly with leaf growth and remained relatively stable through bulb growth and ripening.

This relation between $\sigma^o_{\rm HV}$ and NDVI has limitations. For example, a leaf area index (LAI, $\rm m^2/m^2$) of 0.5 is the commonly

accepted threshold, above which the radar backscatter value is dominated by leaves rather than soil [63], and [9] reported that C-band SAR backscatter was sensitive to crop growth only while $LAI < 4.6$, although this is also dependent on canopy structure due to radar scattering sensitivity. Also, there may be differences in radar backscatter from crops with the same biomass (same NDVI) due to the difference in plant geometry [31]. This is particularly apparent for barley during heading and grain filling [Fig. 5(a)]. As a result, the correlation coefficient between a spline fit to the NDVI measurements (DOY 130–230 at 1-day intervals) with a spline fit of the σ^o_{HV} values was 0.76 and 0.77 for corn and onion, respectively, and only 0.27 for barley. Nonetheless, this relation between σ^o and NDVI is of particular interest because the leaf area is generally assumed to be correlated with final crop yield.

B. Soil Condition

A comparison of irrigated wheat with a nearby field of nonirrigated wheat offers a qualitative insight into the assumption that the radar backscatter from crops with moderate vegetation cover (e.g., $LAI > 0.5$) is dominated by the contribution from vegetation rather than soil moisture or roughness (Fig. 6). In this case, the incidence angle range was limited to 30°–35° because images acquired at 40° and 41° did not include coverage of the nonirrigated wheat field. The nonirrigated wheat field received 57 mm of water from precipitation over the growing season, and the irrigated wheat field received 273 mm of water from irrigation and precipitation. It was estimated that the precipitation and supplemental irrigation in the irrigated wheat field replenished about 60% of the water lost through evapotranspiration (Table III).

First, of interest is the similarity in the time series of backscatter for the two fields. Both time series showed an increase in σ^o_{HH} and σ^o_{HV} associated with leaf growth, a peak σ^o_{HH} and σ^o_{HV} associated with heading, a dramatic drop in σ^o_{HH} and σ^o_{HV} after harvest, and an increase in the $\sigma^o_{\mathrm{VV}} - \sigma^o_{\mathrm{HH}}$ difference with leaf jointing and wheat heading. Second, it was observed that, at the end of the season (after DOY 180), σ^o_{HH} and σ^o_{HV} were lower (more negative) for the irrigated than those for the nonirrigated field due likely to the fact that the nonirrigated field was rougher than the irrigated field. Third, during the period of full cover and irrigation (DOY 100–180), the backscatter from the irrigated wheat was either equal to (σ^o_{HV}) or greater than (σ^o_{HH}) that from the nonirrigated wheat. Although speculative, these results imply that both σ^o_{HH} and σ^o_{HV} are somewhat sensitive to soil moisture content (resulting in σ^o for irrigated wheat greater than or equal to that for nonirrigated wheat) and support the results reported for measurements in an anechoic chamber that, at C-band and at low/moderate incidence angles, the wheat backscatter was responsive to attenuated soil scattering [15]. Nonetheless, in this case (Fig. 6), the trend in σ^o was apparently dominated by the contribution from vegetation rather than the sensitivity to soil moisture differences, i.e., the largest change in backscatter occurred at harvest (going from full cover to stubble) rather than the small differences associated with irrigation and precipitation. However, it should be further noted that wheat stubble has been reported to affect SAR σ^o to an extent determined by the type and amount of residue cover and the radar configuration [36], [37].

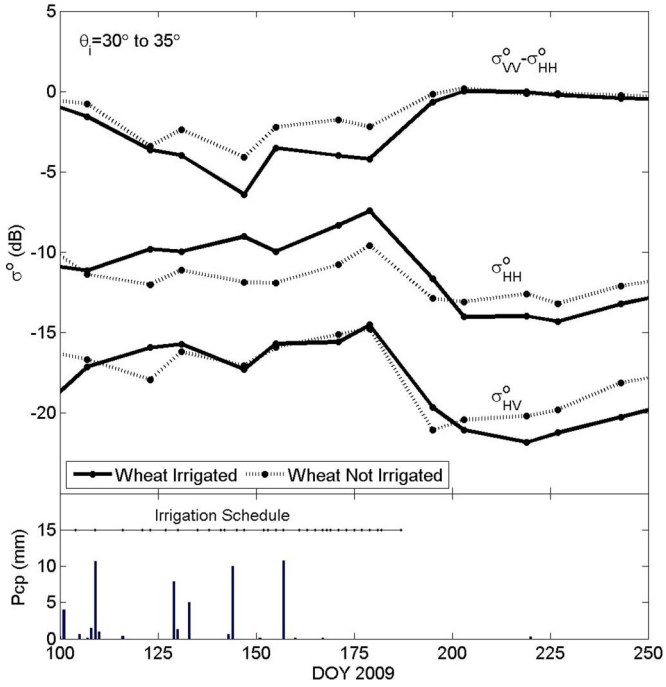

Fig. 6. Comparison of radar backscatter values for irrigated and nonirrigated wheat in HH, HV, and VV-HH polarizations. The symbols represent radar backscatter values for measurements made with ascending and descending orbits with beam incidence angles from 30° to 35°. The lower panel indicates the precipitation associated with the acquisition dates. The irrigation schedule is indicated by a solid line indicating the temporal extent and by dots indicating the irrigation frequency (the daily irrigation amounts varied, and they are not represented here).

C. Relative Sensitivity to Crop/Soil Condition and Satellite/Sensor Configuration

Based on visual interpretation of temporal trends in linearly quad-polarized σ^o (Figs. 3–6), one might conclude that there are three dominant influences on the amplitude of radar backscatter in irrigated crops: soil condition, crop condition, and sensor configuration (view direction and polarization). We have the opportunity here to quantify the behavior and relative dominance of these three influences for irrigated fields of wheat, barley, oat, onion, and corn at Barrax (Fig. 7). For this analysis, we focused on the difference between the dynamic range of $\sigma^o(\Delta\sigma^o)$ for three polarizations and five crops under three conditions:

1) change in soil moisture: analysis of $\Delta\sigma^o$ over 2 days before and after a significant rain event (DOY 238 and 261) when crop change was minimal (grains were already harvested, and corn and onion vegetation were at full cover) and two images were acquired at a steep incidence angle $(\theta_i = 25°)$ [Fig. 7(a)];
2) change in crop vegetation structure: analysis of $\Delta\sigma^o$ over the entire AgriSAR field season (DOY 100–220) when crops were changing dramatically and eight images were acquired at a shallow incidence angle $(\theta_i = 41°)$ [Fig. 7(b)];

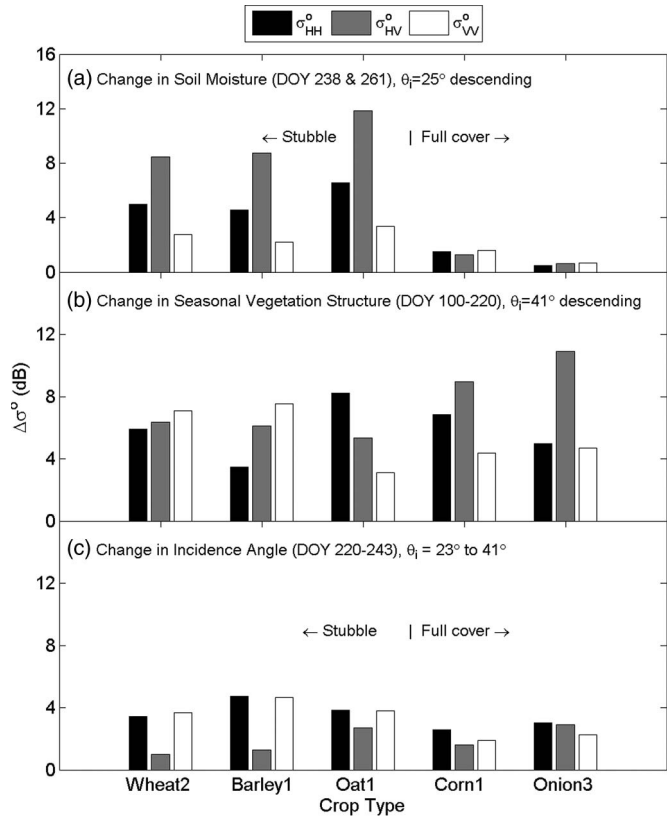

Fig. 7. Difference between maximum and minimum $\sigma^o(\Delta\sigma^o)$ for three polarizations and five crops—wheat, barley, oat, corn, and onion—under three conditions described in the text. (a) Change in soil moisture. (b) Change in crop vegetation structure. (c) Change in beam incidence angle. In frames (a) and (c), the crop growth stage is indicated with text, where cereal crops had been harvested and onion and corn were at full canopy cover. The alfalfa field was excluded from this analysis because it was not covered by the RADARSAT-2 images acquired with $\theta_i = 40^\circ$ or 41°.

3) change in incidence angle: analysis of $\Delta\sigma^o$ over a time period when crop change was minimal and all eight sensor configurations ($\theta_i = 23^\circ - 41^\circ$ and view directions to the left and right of the orbit) were acquired [DOY 220–243; Fig. 7(c)].

Results showed that σ^o at a steep incidence angle was sensitive to precipitation and irrigation events when the crop leaf density was low, particularly in the HV cross-polarization [Fig. 7(a)]. This supports studies suggesting that cross-polarization, rather than copolarization, is a better measure of soil moisture variations (e.g., [35]). The results for corn and onion fields with full-cover vegetation were inconclusive because the fields were being irrigated close to the date of the storm. Unfortunately, there were few opportunities to further investigate the relation between σ^o and soil moisture with the 2009 AgriSAR time series due to the lack of soil moisture measurements during times of irrigation. Analysis was limited to images acquired after the harvest of grain crops and before the leaf development of corn and onion. As such, the AgriSAR analysis at Barrax was focused largely on understanding the value of time series quad-polarized SAR for monitoring crop condition.

Large variations in σ^o at a shallow incidence angle ($\theta_i = 41^\circ$) were associated with changes in crop vegetation structure over the growing season [Fig. 7(b)]. The dynamic range of the HV cross-polarization σ^o_{HV} was consistently high for all crops, ranging from about 6 dB for the grain crops (wheat, barley, and corn) to greater than 8 dB for corn and onion. However, there was also an evidence that the copolarized backscatter might be best in some cases, i.e., the dynamic range of σ^o_{VV} was slightly greater than that for σ^o_{HV} for the wheat and barley fields, and the dynamic range of σ^o_{HH} was greater than that for σ^o_{HV} for the oat field.

Small day-to-day variations in SAR σ^o unrelated to changes in crop and soil conditions were explained by the variations in the RADARSAT-2 satellite/sensor orientation [Fig. 7(c)]. Again, σ^o_{HV} provided the most consistent results across all crops, with a dynamic range less than 4 dB (average 2 dB) for harvested fields of grain and fields with full-cover corn and onion. For these fields at Barrax, there was no apparent trend for the dynamic range associated with incidence angle to be more pronounced in fields of stubble versus fields of full-cover vegetation, as had been reported by others (e.g., [55]).

D. Suggested Image Acquisition Frequency and Polarimetric Mode

A goal of the AgriSAR 2009 campaign was to determine the optimum time interval that would be required in a future satellite system (i.e., Sentinel-1) to provide meaningful information about crop and soil conditions. Sentinel-1 is designed to provide multiple configurations with a constellation of satellites, resulting in acquisitions at a single site every 2 days. With RADARSAT-2, the full repetition cycle is 24 days, which resulted in only 6–8 single-configuration images acquired during the AgriSAR campaign instead of 57 multiconfiguration images. To test if the few images of one satellite/sensor configuration would provide the same seasonal trends as multiple images of eight configurations, we computed the correlation coefficient (R^2) between a spline fit of σ^o_{HV} values measured with all configurations from within the time period DOY 092–234 ($n = 41$ images and frequency $\sim$3 days) with a spline fit of σ^o_{HV} values with only one configuration ($n = 6$ images and frequency $= 24$ days) over the growing season for wheat, barley, oat, corn, onion, and alfalfa fields [Table IV and Fig. 8(a)]. The results showed that the trends differed greatly (resulting in low R^2 value) when crop phenology was changing rapidly or when storms or irrigation occurred when LAI was low because these events were not captured by the 24-day repeat. These events caused some low R^2 values for grain crops (undergoing jointing, heading, and harvest), moderate R^2 values for corn (with steady leaf growth and mid-season tasseling), and the highest R^2 values for onion (which had green vegetation through most of the season, with little change in σ^o_{HV} associated with bulb growth and ripening). The R^2 values for alfalfa were lowest due to the rapid and dramatic decrease in σ^o associated with frequent alfalfa harvests.

The ability of a 24-day acquisition frequency to capture the information of the average 3-day acquisition frequency was apparently dependent upon the crop type, time of year, and timing of the repeat cycle relative to rapidly changing crop and soil conditions [Fig. 8(a)]. To test if finer acquisition frequencies could capture more information, we computed the

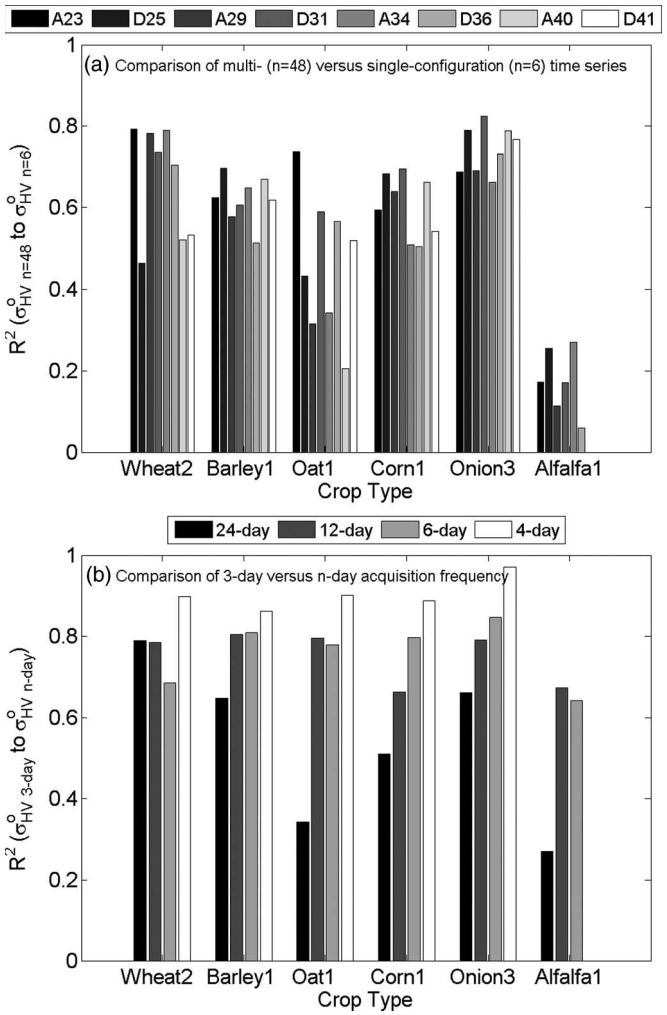

Fig. 8. Correlation coefficient between a spline fit to σ^o_{HV} values over the growing season (within the time period DOY 92–234 at 1-day intervals) for wheat, barley, oat, corn, onion, and alfalfa fields at Barrax (a) for all configurations ($n = 41$ images) and for only one configuration as listed in the legend ($n = 6$ images) and (b) for the average 3-day acquisition frequency and for 24-, 12-, 6-, and 4-day frequencies. Note: the results for the alfalfa field differed from all others because the field was not covered by the RADARSAT-2 images acquired with $\theta_i = 40^\circ$ or 41°. Consequently, for (a), the data for alfalfa at A40 and D41 were not available, and for (b), the 24-, 12-, and 6-day frequencies were compared to the 4-day frequency.

R^2 between a spline fit of σ^o_{HV} values measured at an average 3-day frequency with average 24-, 12-, 6-, and 4-day frequencies within the time period DOY 092–234 [Table IV and Fig. 8(b)]. With an average 6-day acquisition frequency, it was possible to obtain $R^2 \geq 0.6$ for all six crops. Increasing the acquisition frequency to a 4-day average resulted in a substantial increase in the R^2 value to > 0.85 for all crops (alfalfa was excluded because it was not covered by images acquired at $\theta_i = 40^\circ$ or 41°). The occasions when the R^2 showed a slight decrease with increased acquisition frequency (e.g., wheat2, oat1, and alfalfa1 for 6-day frequency) emphasized the importance of both the acquisition frequency and the timing of the acquisitions relative to rapidly changing crop conditions.

Planning a satellite system with the optimal image acquisition frequency and best polarimetric mode depends on the priorities of the mission. Based on this analysis for six crops at Barrax over the 2009 growing season from DOY 92–234, image acquisition frequencies ranging from 1 to 6 days and polarimetric modes from single- to quad-polarized were suggested depending on the goals of the mission (Table V). We found that quad-polarization with image acquisition frequency from 3–6 days was best suited for distinguishing crop types and for monitoring crop phenology, single- or dual-polarization with an acquisition frequency of 3–6 days was sufficient for mapping crop green biomass, and single- or dual-polarization with daily image acquisition was necessary to capture rapid changes in soil moisture condition. For all mission applications, a dense time series (acquisitions every 3–6 days) was required to discriminate variations in surface crop and soil conditions from differences induced by changes in satellite/sensor configuration.

IV. Conclusion

Related to the AgriSAR objective of deriving agricultural information from time series quad-polarized SAR products, it appeared that the temporal trend and overall amplitude of SAR quad-polarized σ^o could be related to crop and soil conditions. More specifically, for this paper, the following conclusions are derived.

1) The SAR backscatter was dominated by the vegetation response, although sensitive to the soil response, throughout most of the growing season.
2) The cross-polarized σ^o_{HV} was particularly useful for monitoring both crop and soil conditions and was found to be the most insensitive to differences in sensor view direction and beam incidence angle. At shallow incidence angles, σ^o_{HV} was the most sensitive polarization to changes in vegetation structure with crop seasonal growth and harvest.
3) The greatest separability of barley, corn, and onion occurred in spring after the barley had been harvested or in the narrow time window associated with grain crop heading when corn and onion were still immature.
4) The time series of σ^o offered reliable information about crop growth stage, such as jointing and heading in grain crops and leaf development and reproduction in corn and onion.
5) There was a positive correlation between RADARSAT-2 σ^o and RapidEye NDVI for onion and corn, where the percentage increase in σ^o was on the same order as the percentage increase in NDVI. This relation was complicated by plant geometry, resulting in a poor σ^o/NDVI relation during certain crop growth stages (e.g., wheat heading) and different σ^o/NDVI relations for different crop structures (barley versus corn versus onion).
6) For a limited study of pre- and postprecipitation conditions, the cross-polarization σ^o_{HV}, rather than copolarization σ^o_{HH} or σ^o_{VV}, was a better measure of soil moisture variation for sparsely vegetated fields.
7) The impact of view direction and incidence angle on the time series was minimal compared to the signal response to crop and soil conditions. Again, σ^o_{HV} had the lowest sensitivity of all polarizations to sensor configurations for crop fields at a variety of green leaf areas at Barrax.

TABLE V
SUGGESTED OPTIMUM ACQUISITION FREQUENCY AND POLARIMETRIC MODE BY MISSION MAPPING GOAL WITH JUSTIFICATION, BASED ON THE BARRAX 2009 ANALYSIS FOR 12 FIELDS OF SIX CROPS. NOTE: SUGGESTED POLARIMETRIC MODES ARE ABBREVIATED, WHERE QUAD-POL REFERS TO LINEAR QUAD-POLARIZATIONS HH+VV+HV+VH, DUAL-POL REFERS TO LINEAR DUAL-POLARIZATIONS HH+HV OR VV+VH, AND SINGLE-POL REFERS TO LINEAR SINGLE-POLARIZATIONS HH, VV, HV, OR VH

Mission Mapping Goal	Suggested Polarimetric Mode	Suggested Acquisition Frequency	Justification
Crop Type		3-6 days	The greatest discrimination of these 6 crops was related to narrow time windows of crop growth stage and harvest (e.g., Figure 4). Acquisitions every 3-6 days should allow 1-2 acquisitions within these windows.
	Quad-Pol		The different responses of σ^o_{HV} and σ^o_{VV}-σ^o_{HH} to growth stages in grain crops and other crops (e.g., Figures 4 and 7), combined with a dense time-series, offered the best opportunities to discriminate crop types.
Crop Growth Stage		3-6 days	Crop growth stage was determined by a significant deviation from the season-long trend of σ^o (e.g., Figure 4). Acquisitions every 3-6 days should provide context for this deviation.
	Quad-Pol		The combined measures of σ^o_{HV} and σ^o_{VV}-σ^o_{HH} provided maximum information about crop phenology due to different sensitivities to crop growth and reproductive stages (e.g., Figures 4 and 6).
Crop Green Biomass		3-6 days	Crop green biomass was positively correlated with σ^o but could be confounded by changes in phenology, soil moisture and soil roughness (e.g., Figure 5). Acquisitions every 3-6 days should discriminate changes in biomass from other soil and crop variations.
	Single- or Dual-Pol		The σ^o_{HV} was the most sensitive measure of green vegetative material (e.g., Figures 3 and 5) due to the depolarizing effect of volumetric scattering within a crop canopy.
Surface Soil Moisture (for LAI<0.5)		Daily	The response of σ^o to surface soil moisture was large but of short duration. Daily acquisition frequency should capture these rapid changes.
	Single- or Dual-Pol		Both σ^o_{HH} and σ^o_{HV} were sensitive to changes in soil moisture, however σ^o_{HV} had the advantages of providing a greater dynamic range and being least sensitive to changes in beam incidence angle (Figure 7).

Related to planning for Sentinel-1, we suggested image acquisition frequencies ranging from 1 to 6 days and polarimetric modes from single- to quad-polarized depending on the goals of the mission (Table V). Furthermore, the noise induced into the time series analysis by including multiple view directions and incidence angles was small compared to the information about crop and soil conditions gained by the dense time series of measurements. These results should be considered with the caveat that the study was limited to six crops with pivot irrigation and specific row direction and soil roughness.

With the knowledge gained in this analysis, the next steps will focus on several aspects. We will conduct a similar analysis of multitemporal quad-polarized data for individual fields at the other two AgriSAR experimental sites—Flevoland and Indian Head. The experiment at Barrax will be repeated to allow an interyear comparison that would enable generalizations to be made [51]. The 2009 RADARSAT-2 time series will be interpreted using a combined crop growth/radar backscatter modeling system supported by available optical images to best utilize the time series information for land monitoring (e.g., [2] and [45]).

REFERENCES

[1] R. G. Allen, L. S. Pereira, D. Raes, and M. Smith, Crop Evapotranspiration. Guidelines for Computing Crop Water Requirements, Rome, 1998, FAO Irrig. Drain. Pap. 56, FAO, 300 pp.

[2] H. Bach and W. Mauser, "Methods and examples for remote sensing data assimilation in land surface process modeling," *IEEE Trans. Geosci. Remote Sens.*, vol. 41, no. 7, pp. 1629–1637, Jul. 2003.

[3] N. Baghdadi, N. Boyer, P. Todoroff, M. El Hajj, and A. Begue, "Potential of SAR sensors TerraSAR-X, ASAR/Envisat and PALSAR/ALOS for monitoring sugarcane crops on Reunion Island," *Remote Sens. Environ.*, vol. 113, no. 8, pp. 1724–1738, Aug. 2009.

[4] A. Balenzano, F. Mattia, G. Satalino, and M. W. J. Davidson, "Dense temporal series of C- and L-band SAR data for soil moisture retrieval over agricultural crops," *IEEE J. Sel. Topics Appl. Earth Observ. Remote Sens.*, vol. 4, no. 2, pp. 439–450, Jun. 2011.

[5] Y. Ban and P. J. Howarth, "Orbital effects on ERS-1 SAR temporal backscatter profiles of agricultural crops," *Int. J. Remote Sens.*, vol. 19, no. 17, pp. 3465–3470, Nov. 1998.

[6] Y. Ban and P. J. Howarth, "Multitemporal ERS-1 SAR data for crop classification: A sequential-making approach," *Can. J. Remote Sens.*, vol. 25, no. 4, pp. 438–447, 1999.

[7] X. Blaes, L. Vanhalle, and P. Defourny, "Efficiency of crop identification based on optical and SAR image time series," *Remote Sens. Environ.*, vol. 96, no. 3/4, pp. 352–365, Jun. 2005.

[8] X. Blaes, F. Holecz, H. J. C. van Leeuwen, and P. Defourny, "Regional crop monitoring and discrimination based on simulated Envisat ASAR wide swath mode images," *Int. J. Remote Sens.*, vol. 28, no. 2, pp. 371–393, Jan. 2007.

[9] X. Blaes, P. Dourny, U. Wegmuller, A. D. Vecchia, L. Guerriero, and P. Ferrazzoli, "C-band polarimetric indexes for maize monitoring based on a validated radiative transfer model," *IEEE Trans. Geosci. Remote Sens.*, vol. 44, no. 4, pp. 791–800, Apr. 2006.

[10] T. W. Brakke, E. T. Kanemasu, J. L. Steiner, F. T. Ulaby, and E. Wilson, "Microwave response to canopy moisture, leaf-area index and dry weight of wheat, corn and sorghum," *Remote Sens. Environ.*, vol. 11, pp. 207–220, 1981.

[11] B. Brisco and R. J. Brown, "Manual of Remote Sensing," in *Agricultural Applications With Radar*, R. A. Ryerson, Ed. Hoboken, NJ: Wiley, 1998, ch. 7, pp. 381–406.

[12] B. Brisco, F. T. Ulaby, and R. Protz, "Improving crop classifications through attention to the timing of airborne radar acquisitions," *Photogram. Eng. Remote Sens.*, vol. 50, no. 6, pp. 739–745, 1984.

[13] B. Brisco, R. J. Brown, B. Snider, G. J. Sofko, J. A. Koehler, and A. G. Wacher, "Tillage effects on the radar backscattering coefficient of grain stubble fields," *Int. J. Remote Sens.*, vol. 12, no. 11, pp. 2283–2298, Nov. 1991.

[14] B. Brisco, R. J. Brown, J. G. Gairns, and B. Snider, "Temporal ground-based scatterometer observations of crops in Western Canada," *Can. J. Remote Sens.*, vol. 18, no. 1, pp. 14–21, 1992.

[15] S. C. M. Brown, S. Quegan, K. Morrison, J. C. Bennett, and G. Cookmartin, "High-resolution measurements of scattering in wheat canopies—Implications for crop parameter retrieval," *IEEE Trans. Geosci. Remote Sens.*, vol. 41, no. 7, pp. 1602–1610, Jul. 2003.

[16] T. F. Bush and F. T. Ulaby, "An evaluation of radar as a crop classifier," *Remote Sens. Environ.*, vol. 7, no. 1, pp. 15–36, 1978.

[17] M. Chakraborty, K. R. Manjunath, S. Panigrahy, N. Kindu, and J. S. Parihar, "Rice crop parameter retrieval using multi-temporal, multi-incidence angle RADARSAT SAR data," *ISPRS J. Photogram. Remote Sens.*, vol. 59, no. 5, pp. 310–322, Aug. 2005.

[18] P. de Matthaeis, G. Schiavon, and D. Solimini, "Effect of scattering mechanisms on polarimetric features of crops and trees," *Int. J. Remote Sens.*, vol. 15, no. 14, pp. 2917–2930, 1994.

[19] F. Del Frate, G. Schiavon, D. Solimini, M. Borgeaud, D. H. Hoekman, and M. A. M. Vissers, "Crop classification using multiconfiguration C-band SAR data," *IEEE Trans. Geosci. Remote Sens.*, vol. 41, no. 7, pp. 1611–1619, Jul. 2003.

[20] J. Doorenbos and W. O. Pruitt, Guidelines for Predicting Crop Water Requirements, Rome, 1977. FAO Irrig Drain Pap 24, FAO, 144 pp.

[21] P. Ferrazzoli, L. Guerriero, and G. Schiavon, "Experimental and model investigation on radar classification capability," *IEEE Trans. Geosci. Remote Sens.*, vol. 37, no. 2, pp. 960–968, Mar. 1999.

[22] G. M. Foody, M. B. McCulloch, and W. B. Yates, "Crop classification for C-band polarimetric radar data," *Int. J. Remote Sens.*, vol. 15, no. 14, pp. 2871–2885, 1994.

[23] I. Hajnsek, R. Horn, R. Scheiber, R. Bianchi, and M. Davidson, "The AgriSAR campaign: Monitoring the vegetation cycle using polarimetric SAR data," in *Proc. Envisat Symp.*, Montreux, Switzerland, Apr. 23–27, 2007.

[24] J. L. Hatfield and P. J. Pinter, Jr., "Remote sensing for crop protection," *Crop Protect.*, vol. 12, no. 6, pp. 403–413, Sep. 1993.

[25] H. Hirosawa, S. Komiyama, and Y. Matsuzaka, "Cross-polarized radar backscatter from moist soil," *Remote Sens. Environ.*, vol. 7, no. 3, pp. 211–217, Aug. 1978.

[26] P. Hoogeboom, "Classification of agricultural crops in radar images," *IEEE Trans. Geosci. Remote Sens.*, vol. GE-21, no. 3, pp. 329–336, Jul. 1983.

[27] R. D. Jackson, "Remote sensing of vegetation characteristics for farm management," in *Proc. SPIE—Int. Soc. Opt. Eng.*, 1984, vol. 475, pp. 81–96.

[28] T. Le Toan, H. Laur, E. Mougin, and A. Lopes, "Multi-temporal and dual-polarization observations of agricultural vegetation covers by X-band SAR images," *IEEE Trans. Geosci. Remote Sens.*, vol. 27, no. 6, pp. 709–718, Nov. 1989.

[29] L. Liu, J. Wang, Y. Bao, W. Huang, Z. Ma, and C. Zhao, "Predicting winter wheat condition, grain yield and protein content using multi-temporal Envisat-ASAR and Landsat TM satellite images," *Int. J. Remote Sens.*, vol. 27, no. 4, pp. 737–753, Feb. 2006.

[30] R. López-Urrea, F. Martín de Santa Olalla, C. Fabeiro, and A. Moratalla, "Testing evapotranspiration equations using lysimeter observations in a semiarid climate," *Agric. Water Manage.*, vol. 85, no. 1/2, pp. 15–26, Sep. 2006.

[31] G. Macelloni, S. Paloscia, P. Pampaloni, F. Marliani, and M. Gai, "The relationship between the backscattering coefficient and the biomass of narrow and broad leaf crops," *IEEE Trans. Geosci. Remote Sens.*, vol. 39, no. 4, pp. 873–884, Apr. 2001.

[32] R. Mathieu, M. Sbih, A. A. Viau, F. Anctil, L. E. Parent, and J. Boisvert, "Relationships between RADARSAT SAR data and surface moisture content of agricultural organic soils," *Int. J. Remote Sens.*, vol. 24, no. 24, pp. 5265–5281, Dec. 2003.

[33] F. Mattia, G. Satalino, L. Dente, and G. Pasquariello, "Using a priori information to improve soil moisture retrieval from Envisat ASAR AP data in semiarid regions," *IEEE Trans. Geosci. Remote Sens.*, vol. 44, no. 4, pp. 900–912, Apr. 2006.

[34] F. Mattia, T. Le Toan, G. Picard, F. I. Posa, A. D'Alessio, C. Notarnicola, A. M. Gatti, M. Rinaldi, G. Satalino, and G. Pasquariello, "Multitemporal C-band radar measurements on wheat fields," *IEEE Trans. Geosci. Remote Sens.*, vol. 41, no. 7, pp. 1551–1560, Jul. 2003.

[35] H. McNairn and B. Brisco, "The application of C-band polarimetric SAR for agriculture: A review," *Can. J. Remote Sens.*, vol. 30, no. 3, pp. 525–542, 2004.

[36] H. McNairn, C. Duguay, J. Boisvert, E. Huffman, and B. Brisco, "Defining the sensitivity of multi-frequency and multi-polarized radar backscatter to post-harvest crop residue," *Can. J. Remote Sens.*, vol. 27, no. 3, pp. 247–263, 2001.

[37] H. McNairn, C. Duguay, B. Brisco, and T. J. Pultz, "The effect of soil and crop residue characteristics on polarimetric radar response," *Remote Sens. Environ.*, vol. 80, no. 2, pp. 308–320, May 2002.

[38] H. McNairn, J. Ellis, J. J. Van der Sanden, T. Hirose, and R. J. Brown, "Providing crop information using RADARSAT-1 and satellite optical imagery," *Int. J. Remote Sens.*, vol. 23, no. 5, pp. 851–870, 2002.

[39] H. McNairn, K. Hochheim, and N. Rabe, "Applying polarimetric radar imagery for mapping the productivity of wheat crops," *Can. J. Remote Sens.*, vol. 30, no. 3, pp. 517–524, 2004.

[40] H. McNairn, S. Liali, J. Xianfeng, and C. Champagne, "The contribution of ALOS PALSAR multipolarization and polarimetric data to crop classification," *IEEE Trans. Geosci. Remote Sens.*, vol. 47, no. 12, pp. 3981–3992, Dec. 2009.

[41] M. S. Moran, A. Vidal, D. Troufleau, Y. Inoue, and T. A. Mitchell, "Ku- and C-band SAR for discriminating agricultural crop and soil conditions," *IEEE Trans. Geosci. Remote Sens.*, vol. 36, no. 1, pp. 265–272, Jan. 1998.

[42] M. S. Moran, D. C. Hymer, J. Qi, and E. E. Sano, "Soil moisture evaluation using multitemporal synthetic aperture radar (SAR) in semiarid rangeland," *J. Agric. Forest Meteorol.*, vol. 105, no. 1–3, pp. 69–80, 2000.

[43] M. S. Moran, D. C. Hymer, J. Qi, and Y. Kerr, "Comparisons of ERS-2 SAR and Landsat TM imagery for monitoring agricultural crop and soil conditions," *Remote Sens. Environ.*, vol. 79, no. 2, pp. 243–252, Feb. 2002.

[44] L. C. Morena, K. V. James, and J. Beck, "An introduction to the RADARSAT-2 mission," *Can. J. Remote Sens.*, vol. 30, no. 3, pp. 221–234, Jun. 2004.

[45] G. S. Nearing, M. S. Moran, C. H. Collins, K. R. Thorp, and S. C. Slack, "An improved strategy for assimilating synthetic aperture radar imagery into modeled estimations of soil moisture through parameter optimization," *Remote Sens. Environ.*, vol. 114, pp. 2564–2574, 2010.

[46] P. E. O'Neill, N. S. Chauhan, and T. J. Jackson, "Use of active and passive microwave remote sensing for soil moisture estimation through corn," *Int. J. Remote Sens.*, vol. 17, no. 10, pp. 1851–1865, 1996.

[47] S. Paloscia, "A summary of experimental results to assess the contribution of SAR for mapping vegetation biomass and soil moisture," *Can. J. Remote Sens.*, vol. 28, no. 2, pp. 246–261, 2002.

[48] S. Panigrahy, K. R. Manjunath, M. Chakraborty, N. Kundu, and J. S. Parihar, "Evaluation of RADARSAT standard beam data for identification of potato and rice crops in India," *ISPRS J. Photogram. Remote Sens.*, vol. 54, no. 4, pp. 254–262, Sep. 1999.

[49] J. F. Paris, "The effect of leaf size on the microwave backscattering by corn," *Remote Sens. Environ.*, vol. 19, no. 1, pp. 81–95, Feb. 1986.

[50] A. Rosenqvist, "Temporal and spatial characteristics of irrigated rice in JERS-1 L-band SAR data," *Int. J. Remote Sens.*, vol. 20, no. 8, pp. 1567–1587, May 1999.

[51] P. Saich and M. Borgeaud, "Interpreting ERS SAR signatures of agricultural crops in Flevoland, 1993–1996," *IEEE Trans. Geosci. Remote Sens.*, vol. 38, no. 2, pp. 651–657, Mar. 2000.

[52] G. Satalino, F. Mattia, T. Le Toan, and M. Rinaldi, "Wheat crop mapping by using ASAR AP data," *IEEE Trans. Geosci. Remote Sens.*, vol. 47, no. 2, pp. 527–530, Feb. 2009.

[53] C. G. J. Schotten, W. W. L. Van Rooy, and L. L. F. Janssen, "Assessment of the capabilities of multi-temporal ERS-1 SAR data to discriminate between agricultural crops," *Int. J. Remote Sens.*, vol. 16, no. 14, pp. 2619–2637, 1995.

[54] K. S. Shanmugan, F. T. Ulaby, V. Narayanan, and C. Dobson, "Identification of corn fields using multidate radar data," *Remote Sens. Environ.*, vol. 13, no. 3, pp. 251–264, Jul. 1983.
[55] H. Skriver, M. T. Svendsen, and A. G. Thomsen, "Multitemporal C- and L-band polarimetric signatures of crops," *IEEE Trans. Geosci. Remote Sens.*, vol. 37, no. 5, pp. 2413–2429, Sep. 1999.
[56] H. Skriver, F. Mattia, G. Satalino, A. Balenzano, V. R. N. Pauwels, N. E. C. Verhoest, and M. Davidson, "Crop classification using short-revisit multitemporal SAR data," *IEEE J. Sel. Topics Appl. Earth Observ. Remote Sens.*, vol. 4, no. 2, pp. 423–431, Jun. 2011.
[57] S. Srivastava, S. Cote, S. Muir, and R. Hawkins, "The RADARSAT-1 imaging performance, 14 years after launch, and independent report on RADARSAT-2 image quality," in *Proc. IEEE Geosci. Remote Sens. Symp.*, Honolulu, HI, 2010, pp. 3458–3461.
[58] K. A. Stankiewicz, "The efficiency of crop recognition on Envisat ASAR images in two growing seasons," *IEEE Trans. Geosci. Remote Sens.*, vol. 44, no. 4, pp. 806–814, Apr. 2006.
[59] D. Thoma, M. S. Moran, R. Bryant, M. Rahman, C. D. H. Collins, T. O. Keefer, R. Noriega, I. Osman, S. M. Skirvin, M. Tischler, D. Bosch, P. J. Starks, and C. Peters-Lidard, "Appropriate scale of soil moisture retrieval from high-resolution radar imagery for bare and minimally vegetation soils," *Remote Sens. Environ.*, vol. 112, no. 2, pp. 403–414, Feb. 2008.
[60] D. Thoma, M. S. Moran, R. Bryant, M. Rahman, C. D. H. Collins, S. M. Skirvin, E. E. Sano, and K. Slocum, "Comparison of four models for determining surface soil moisture from C-band radar imagery," *Water Resour. Res.*, vol. 42, no. 1, pp. W01418-1–W01418-12, 2005.
[61] B. Tso and P. M. Mather, "Crop discrimination using multi-temporal SAR imagery," *Int. J. Remote Sens.*, vol. 20, no. 12, pp. 2443–2460, 1999.
[62] F. T. Ulaby and T. F. Bush, "Monitoring wheat growth with radar," *Photogram. Eng. Remote Sens.*, vol. 42, no. 4, pp. 557–568, Apr. 1976.
[63] F. T. Ulaby, C. T. Allen, G. Eger, and K. Kanemasu, "Relating the microwave backscattering coefficient to leaf area index," *Remote Sens. Environ.*, vol. 14, no. 1–3, pp. 113–133, Jan. 1984.
[64] F. T. Ulaby, R. K. Moore, and A. K. Fung, *Microwave Remote Sensing: Active and Passive*, vol. III, *From Theory to Application*. Dedham, MA.: Artech House, 1986.
[65] D. Wang, H. Lin, J. Chen, Y. Zhang, and Q. Zeng, "Application of multi-temporal Envisat ASAR data to agricultural area mapping in the Pearl River Delta," *Int. J. Remote Sens.*, vol. 31, no. 6, pp. 1555–1572, Mar. 2010.

M. Susan Moran received the Ph.D. degree in soil and water science from the University of Arizona, Tucson, in 1990.

She is currently a Hydrologist with the USDA Southwest Watershed Research Center, Tucson. She also holds an adjunct faculty appointment with the Department of Soil, Water and Environmental Science, University of Arizona, and is serving on the NASA Soil Moisture Active Passive Science Definition Team. Her research is focused on arid and semiarid regions, with a broad focus on the impact of land use and climate change on natural resources management and a specialized focus on the application of remote sensing.

Luis Alonso received the B.Sc. degree in physics and the M.Sc. degree in environmental physics (while working on the geometric correction of airborne and spaceborne remote sensing imagery) from the University of Valencia, Valencia, Spain, in 1999 and 2002, respectively.

He is a member of the Laboratory for Earth Observation, Image Processing Laboratory, University of Valencia, where he studies remote sensing of chlorophyll fluorescence at the canopy level. He has participated in several preparatory studies for FLEX candidate mission for ESA's Earth Explorers as well as for GMES Sentinel-2 and Sentinel-3.

Jose F. Moreno received the Ph.D. degree in theoretical physics from the University of Valencia, Valencia, Spain.

He is currently a Professor of earth physics with the Faculty of Physics and the Head of the Laboratory for Earth Observation, Image Processing Laboratory–Scientific Park, University of Valencia. He is working on different national and international projects related to remote sensing and space research and on the development of data processing algorithms and multisource data integration studies, including optical/microwave synergy and imaging spectrometer data processing, for the modeling and monitoring of land surface processes, with special interest in numerical techniques for model inversion and data assimilation applied to remote sensing data. In 1995–1996, he was a Visiting Scientist with the NASA/Jet Propulsion Laboratory, Pasadena, CA. He has been involved in several European research networks and ESA and EC research projects. He is also involved in the Spanish mission SEOSAT within the ESA GMES programme, as chairman of the SEOSAT/Ingenio Mission Advisory Group. He has participated actively in the design and development of several experimental campaigns and studies within preparatory activities for several space missions. He coordinated the proposal for the Fluorescence Explorer (FLEX), a candidate ESA Earth Explorer Mission, and he is currently the Chairman of the FLEX Mission Advisory Group. He is regularly teaching remote sensing courses at the University of Valencia, including Ph.D. courses and Masters on remote sensing, space technologies, and applications. He is the author of many publications in the field, including several book chapters.

Dr. Moreno is a member of the European Space Agency Earth Sciences Advisory Committee, the International Space Station Users Panel, and other scientific advisory committees. He has served as an Associate Editor of the IEEE TRANSACTIONS ON GEOSCIENCE AND REMOTE SENSING.

Maria Pilar Cendrero Mateo received the M.S. degree from the University of Valencia, Valencia, Spain, in 2010. She is currently working toward the Ph.D. degree in the Department of Soil, Water and Environmental Sciences, University of Arizona, Tucson.

Her research is focused on plant fluorescence, with application to crop production and methods of remote sensing.

D. Fernando de la Cruz received the M.S. degree as an Agricultural Engineer from the Technical University of Madrid, Madrid, Spain, in 2000.

He is currently with the irrigation advisory service of the Provincial Agricultural Technical Institute (ITAP) in Albacete, Spain. His area of research is focused on the application of remote sensing for crop and water resources management in semiarid regions.

Amelia Montoro received the Ph.D. degree in agronomics from the University of Castilla La Mancha, Ciudad Real, Spain, in 2008.

She is currently a Postdoctoral Fellow with the South Australian Research and Development Institute, Adelaide, Australia. Her postdoctoral study is on the impact of temperature and water in grapevines. She is an Agronomist with the Instituto Técnico Agronómico Provincial (ITAP), Albacete, Spain, and also a Lecturer with the International Master of Irrigation Program of the Ministry of Agriculture in Spain. Her research interests are in the areas of irrigation scheduling, irrigation science, plant physiology, remote sensing, and farmers' technology transfer.